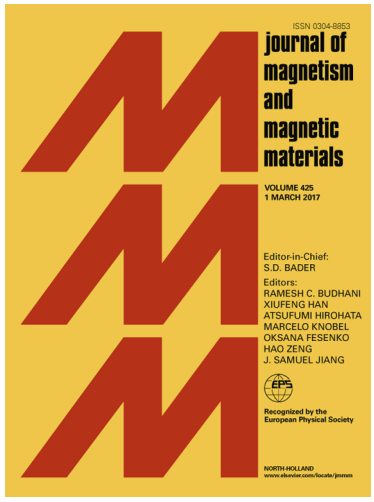

Magnetic properties of ilmenite Mn_2FeSbO_6

Rainer Schmidt

PII: S0304-8853(19)30275-6
DOI: https://doi.org/10.1016/j.jmmm.2019.02.047
Reference: MAGMA 64966

To appear in: *Journal of Magnetism and Magnetic Materials*

Received Date: 21 January 2019
Accepted Date: 16 February 2019

Please cite this article as: R. Schmidt, Magnetic properties of ilmenite Mn_2FeSbO_6, *Journal of Magnetism and Magnetic Materials* (2019), doi: https://doi.org/10.1016/j.jmmm.2019.02.047

Magnetic properties of ilmenite Mn_2FeSbO_6

Rainer Schmidt[a,b]*

[a] *Universidad Complutense de Madrid, GFMC, Dpto. Física de Materiales, Facultad de Ciencias Físicas, 28040 Madrid, Spain*

[b] *Unidad Asociada "Laboratorio de heteroestructuras con aplicación en spintrónica", UCM- CSIC, Sor Juana Ines de la Cruz, 3, Cantoblanco E-28049 Madrid, Spain*

*Corresponding author. Electronic mail: rainerxschmidt@googlemail.com

Magnetic properties of ilmenite Mn_2FeSbO_6

Abstract

In the work presented the magnetic properties of the high pressure ilmenite phase Mn_2FeSbO_6 are investigated in detail. It is shown that Mn_2FeSbO_6 ilmenite is ferrimagnetic ($T_N \approx 270$ K) and exhibits a near-zero coercive field H_C. Furthermore, the Mn^{2+}-Mn^{2+}, Fe^{3+}-Fe^{3+} and Mn^{2+}-Fe^{3+} magnetic exchange interactions exhibit gradual and continuous variations with temperature and magnetic field. The ferrimagnetic moment is unsaturated even at 120 kOe below the theoretical value of 5 μ_B per f.u.

Keywords

Multiferroics; Magnetism; Superparamagnetism; Ilmenite;

Highlights

- Discussion of the crystal and magnetic structure of ilmenite Mn_2FeSbO_6
- Ferrimagnetic transition at $T_N = 270$ K
- Identical zero field and field cooled (ZFC-FC) M vs T curves
- Significant changes in M vs T curves with H and T due to unsaturated moments
- Near-zero coercive field in magnetization M vs applied magnetic field H curves

1. Introduction

Multiferroic materials exhibit two or more ferroic properties for potential application in the electronics industry [1, 2]. This is particularly promising in materials where ferroelectricity and ferromagnetism coexist. In reality, only few materials are known where ferroelectricity and ferromagnetism occur in one single phase and it has been argued that the two properties are mutually exclusive in single oxide materials [3, 4].

The few known single phase multiferroics are binary or more complex oxides that may be classified into two categories [5]: In type-I multiferroics, ferroelectricity and ferromagnetism arise from two independent mechanisms, whereas in type-II multiferroics ferroelectricity is a direct consequence of the magnetic order. Type-I multiferroicity occurs in materials like $BiFeO_3$ [6-10], $BiMnO_3$ [11-14] and related compounds [15-18] with relatively high ordering temperatures, which often come at the expense of small magnetoelectric coupling (MEC) effects. In type-II multiferroics the intrinsic connection of ferroelectric order to the magnetic one is expected to produce large MEC, but such ferroic properties tend to order at lower temperatures [19-21].

Recently, significant progress has been reported of large MEC at ≈ 260 K in ilmenite Mn_2FeSbO_6 polycrystals [22]. The MEC effect is manifested by a large peak in the curves of the real part of the dielectric permittivity ε' vs temperature (T), where the peak appears at $T \approx 260$ K under low applied magnetic field (H) just below the ferrimagnetic transition T_N and is absent at $H = 0$. Furthermore, a relaxor-like ferroelectric transition was detected at $T \approx 650$ K in form of a large frequency dependent peak in ε' vs T curves, and a satellite peak is displayed at lower T at ≈ 500 K reminiscent of a second ferroelectric transition [22]. Therefore, ilmenite Mn_2FeSbO_6 may be regarded a type-I multiferroic material with

independent (anti-)ferroelectric ($T_C \approx 500$ K / 650 K) and ferrimagnetic ($T_N \approx 270$ K) order exhibiting unusually strong MEC. Although a preliminary model for the MEC mechanism was proposed [22], clear experimental evidence is still lacking. Here in this work a detailed study of the magnetic properties in ilmenite Mn_2FeSbO_6 is presented, which may constitute a first step towards the development of a more detailed understanding of the MEC effect in this material.

2. Ilmenite Mn_2FeSbO_6

The ilmenite Mn_2FeSbO_6 phase is a high pressure mineral, which was first called melanostibian upon its discovery by L.J. Igelström in 1892 in the manganese ore mine of Sjögrufvan (Sweden) [23, 24]. The mineral was renamed to melanostibite in 1968 by P.B. Moore [25, 26] and produced first in its synthetic form under high pressure in 1996 [27]. The magnetism and the ferrimagnetic transition at $T_N \approx 270$ K were first investigated by R. Mathieu et al. in 2011 [28], whereas Hudl et al. discovered a magnetocaloric effect at T_N [29]. More recently, the Ti-doped variants $Mn_3FeTiSbO_9$ and $Mn_4FeTi_2SbO_{12}$ have been found to crystallize in the ilmenite structure without the application of high pressure [30, 31].

The ABO_3 ilmenite structure corresponds to a stacked corundum as demonstrated in Figure 1a. The stacked A-site Mn^{2+} and B-site Sb^{5+}/Fe^{3+} (001) ***c***-planes are perpendicular to and align along the [001] ***c***-crystal direction, where the Sb^{5+}/Fe^{3+} cations are randomly distributed within one plane, i.e cation ordering is absent. Along the ***c***-crystal direction the stacking sequence is Mn^{2+} - Sb^{5+}/Fe^{3+} - □ - Sb^{5+}/Fe^{3+} - Mn^{2+} - □ - Mn^{2+}, i.e. with an occupancy of 2/3, where □ denotes a vacant site. The octahedral VI-coordinated A- and B-cationic sites are crystallographically similar but not identical due to different octahedral

tilting angles. The (001) Mn^{2+} and Sb^{5+}/Fe^{3+} ***c***-planes are indicated in Figure 1 by orange and green color respectively. The oxygen octahedra within one plane are edge shared, but alternatingly share a face with an octahedron from one of the neighboring planes and three corners with a total of six octahedra from the other opposite neighboring plane (Figure 1a).

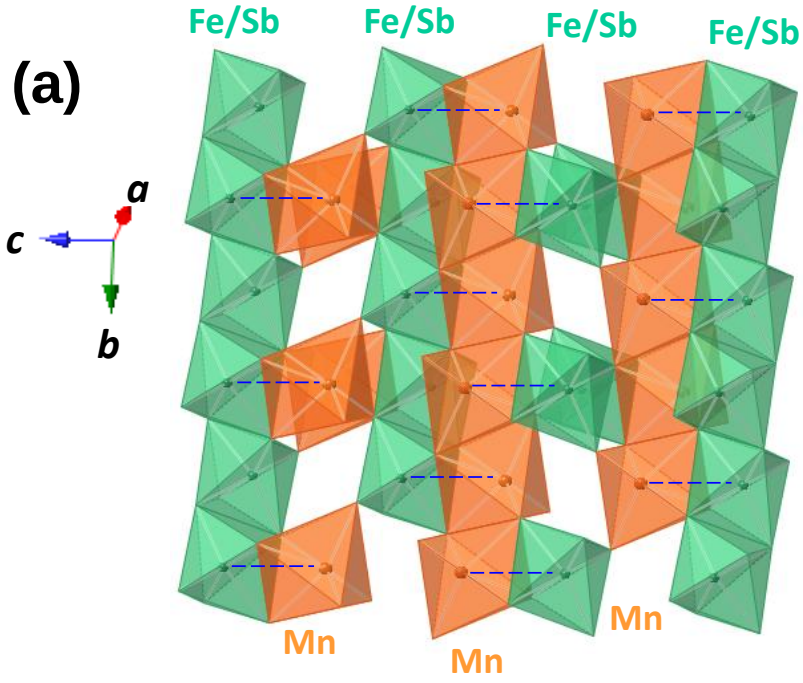

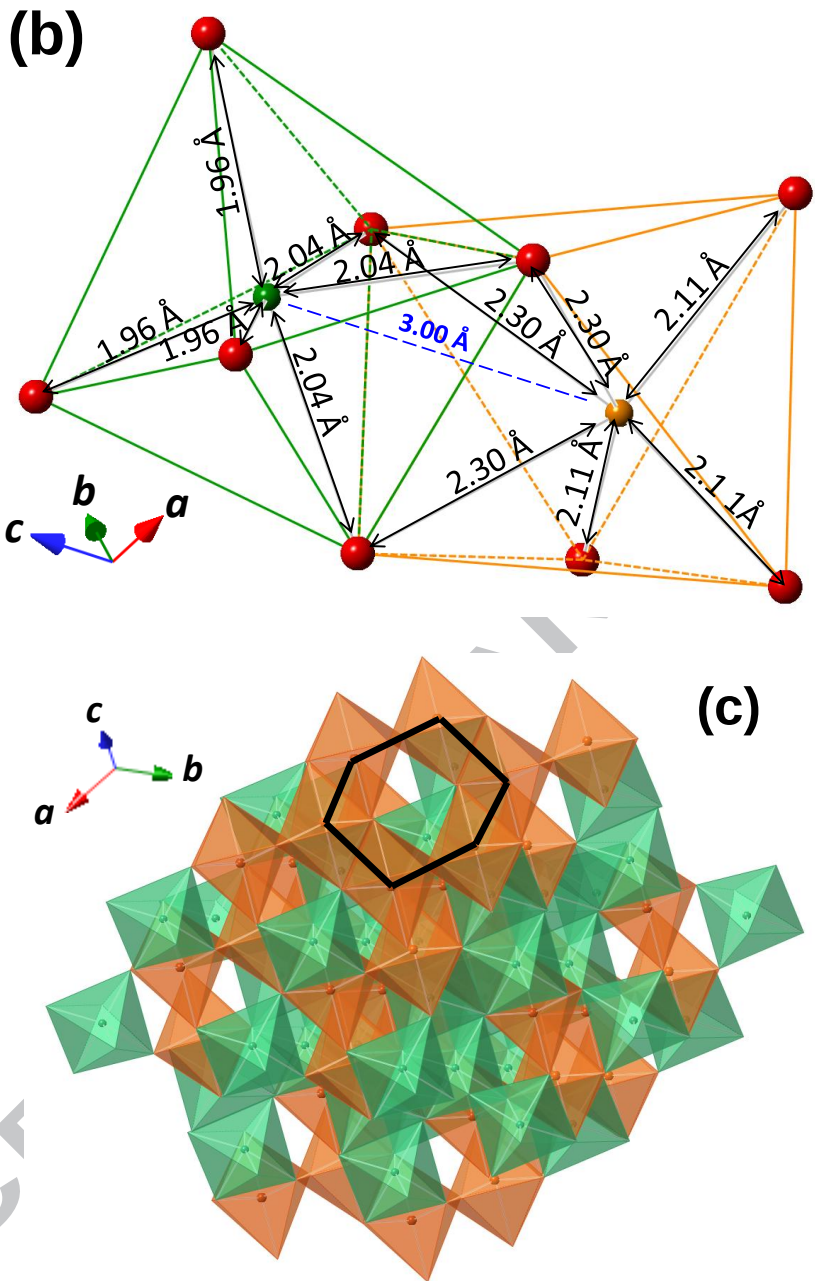

Figure 1 Crystal structure of ilmenite Mn_2FeSbO_6 according to [25]: **(a)** Structural [110] projection. The stacking of Mn-Sb/Fe cation layers along the [001] ***c***-direction is indicated. **(b)** Cations are slightly shifted from the octahedral centers as indicated by slightly different Mn-O and Fe/Sb – O bonding distances due to Coulomb repulsions between Mn^{2+} and

Fe^{3+}/Sb^{5+} cation pairs, indicated by blue dashed lines. **(c)** Hexagonal arrangement of the octahedra within the (001) ***c***-planes demonstrating the vacant sites □.

Due to Mn^{2+} and Sb^{5+}/Fe^{3+} Coulomb repulsions in the face sharing octahedra (indicated by blue dashed lines in Figure 1 a & b) an off-centering and displacement of all cations from their central octahedral positions is indicated in Figure 1b by slightly different Mn-O and Fe/Sb – O bond length [25]. This gives rise to alternating displacements of the Mn^{2+} and Fe^{3+}/Sb^{5+} cations above and below the (001) planes. The oxygen octahedra within one plane exhibit a hexagonal arrangement with an occupancy of 2/3 as depicted in Figure 1c and the structure can be represented by hexagonal sub-cells (Figure 2).

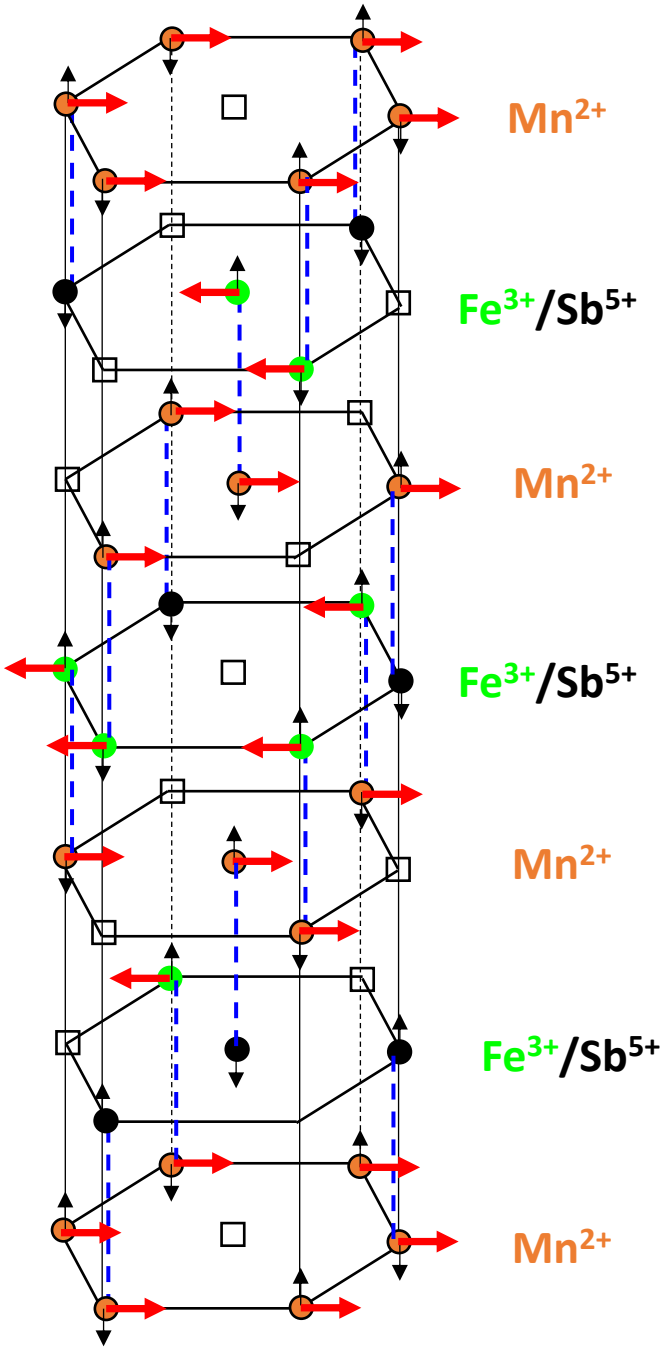

Figure 2 Hexagonal sub-cells of Mn_2FeSbO_6 ilmenite. The magnetic spin exchange interactions between isoelectronic Mn^{2+} cations (orange spheres) and Fe^{3+} (green) are depicted. Non-magnetic Sb^{5+} cations are shown in black, □ are vacant sites. Red arrows indicate possible spin orientations and black arrows show the cationic displacements due to Coulomb repulsions (blue dashed lines).

In previous research, the magnetic interactions of the cations within and between the ***c***-planes were predicted from comparison with ilmenite $NiMnO_3$ and from theoretical considerations: (a) ferromagnetic Mn^{2+} - Mn^{2+}, (b) ferromagnetic Fe^{3+}-Fe^{3+}, which are interrupted by non-magnetic Sb^{5+} [28, 32], and (c) antiferromagnetic Mn^{2+} - Fe^{3+} (Figure 2). It should be noted though that the predicted ferromagnetic Mn^{2+} - Mn^{2+} interactions in Mn_2FeSbO_6 contradict the case of $MnTiO_3$ ilmenite, which is one of the most studied A-site Mn^{2+} ilmenites [33-36] showing antiferromagnetic A-site ordering of Mn^{2+} - Mn^{2+} cations. Also in ilmenite $NiTiO_3$, A-site antiferromagnetic order had been reported [33, 37]. The prediction of ferromagnetic B-site ordering of Fe^{3+}-Fe^{3+} is in agreement though with the case of corundum α-Fe_2O_3 ferrite, where Fe^{3+} cations on the B-sites show in-plane ferromagnetism [38, 39], as well as on the A-sites, and the Fe^{3+} - Fe^{3+} interactions between different A-site/B-site planes are antiferromagnetic. Therefore, it may be plausible that in ilmenite Mn_2FeSbO_6, the B-site Fe^{3+} - Fe^{3+} interactions are ferromagnetic, and A-site/B-site interactions between isoelectronic Mn^{2+} - Fe^{3+} antiferromagnetic (Figure 2). The predicted ferrimagnetic moment is 5 μ_B per formula unit f.u. (Mn_2FeSbO_6).

Interestingly, the Fe^{3+} - Fe^{3+} spins at different A-site/B-site planes in α-Fe_2O_3 are not perfectly aligned antiferromagnetically and give rise to a small net magnetic moment above the well-known Morin transition at T_M = 260 K [40, 41]. By cooling below T_M the net magnetic moment disappears, the spins reorient from lying within the ***c***-plane to an orientation along the ***c***-crystal direction and are perfectly compensated antiferromagnetically. On the other hand, for smaller particle sizes T_M decreases, the spins fluctuate within the ***c***-plane below T_M and superparamagnetism occurs [41, 42].

To predict the strength of different magnetic interactions in Mn_2FeSbO_6 it is convenient that iso-electronic Mn^{2+} and Fe^{3+} cations possess exclusively half-filled *d*-orbitals leading to antiferromagnetic super-exchange according to the Goodenough-Kanamori rules, and Sb^{5+} are non-magnetic. On the other hand, due to the Mn^{2+} - O^{2-} - Fe^{3+} bonding angles being near 90°, direct ferromagnetic exchange interactions may occur in addition to super-exchange and the two mechanisms may compete with each other. In fact, the different B-site/B-site (ferromagnetic) and A-site/B-site (antiferromagnetic) interactions may be understood by dominating direct exchange or super-exchange interactions respectively.

The strongest overall exchange interactions on a local level may be between Mn^{2+} - Fe^{3+} in face-sharing octahedra with the smallest atomic distance (≈ 3.01 Å) of all cationic pairs (see blue dashed lines in Figure 1 a & b). On the other hand, all long-range magnetic interactions involving B-site Fe^{3+} cations are diluted by Sb^{5+} on a macroscopic level and the strongest long-range magnetic order may occur between Mn^{2+} - Mn^{2+} A-site cations with a distance of ≈ 3.14 Å.

3. Experimental

In this work the same ilmenite Mn_2FeSbO_6 polycrystals of the R-3 space group were analyzed that had been used previously for dielectric measurements in reference [22]. The synthesis had been carried out in a platinum pressure cell within a Conac-type press at high pressure (3 GPa) at 1200 °C for 12 min using Mn_2O_3, Fe_2O_3 and Sb_2O_3 precursors [22]. A Quantum Design SQUID MPMS was used to measure the magnetic susceptibility χ vs T at 5 K - 320 K during heating under ZFC and FC conditions under various applied magnetic fields H (20 Oe - 10 kOe). Before applying low H of 20 Oe, the MPMS magnetic coil was

carefully demagnetized by cycling H around zero several times at T = 300 K above T_N. Magnetization (M) vs H curves were measured by cycling H between + 50 kOe and - 50 kOe at 5 K - 300 K. Since the M vs H curves showed no saturation even at 50 kOe, additional M vs H curves were collected by cycling H between +120 kOe and -120 kOe at 50 K - 250 K.

4. Results and discussion

Figure 3 shows the T-dependence of the susceptibility χ (emu mol^{-1} Oe^{-1}) for different applied H (Oe), measured under ZFC and FC conditions as indicated. The highest values of χ measured are all in the range of 8 – 10 emu $mol^{-1}Oe^{-1}$ for small H up to 1 kOe, which implies that the sample magnetization is not saturated and increases approximately linear with H. At higher H the maximum χ values decrease rapidly, indicative of a saturation effect, where this saturation effect is also obvious at the low-T end of the curves for H = 5 kOe and 10 kOe.

The local maxima or peaks in the χ vs T curves shown in Figure 3 move towards lower T for applied H of 20 Oe,100 Oe, 500 Oe and 1 kOe from ≈ 260 K to ≈ 255 K to 175 K and 115 K, respectively. At 5 kOe and 10 kOe no peaks in χ vs T are displayed and the saturation effect mentioned above is evident at low T. The peak in χ vs T for lower H indicates a gradual loss or weakening of the ferrimagnetic order towards lower T, which may be reminiscent of a spin glass behavior. However, the approximately identical behavior of χ vs T under ZFC and FC conditions would exclude a typical spin glass scenario, because ZFC and FC curves would be expected to deviate from each other near the spin glass transition and FC curves would be expected to exhibit no peak at all [28].

Therefore, the magnetic behavior observed here may alternatively be interpreted by *H*- and *T*-dependent variations in the different Mn^{2+}-Mn^{2+}, Fe^{3+}-Fe^{3+} and Mn^{2+}-Fe^{3+} magnetic exchange interactions, possibly involving a varying degree of spin canting and competition between direct- and super-exchange. Similar magnetic behavior had been detected before in systems with at least 3 competing magnetic exchange interactions such as rare-earth (RE)-doped chromites [43-47]. The balance between the competing interactions may be subtle, and external stimuli like varying *H* and *T* may lead to variations in the spin orientations.

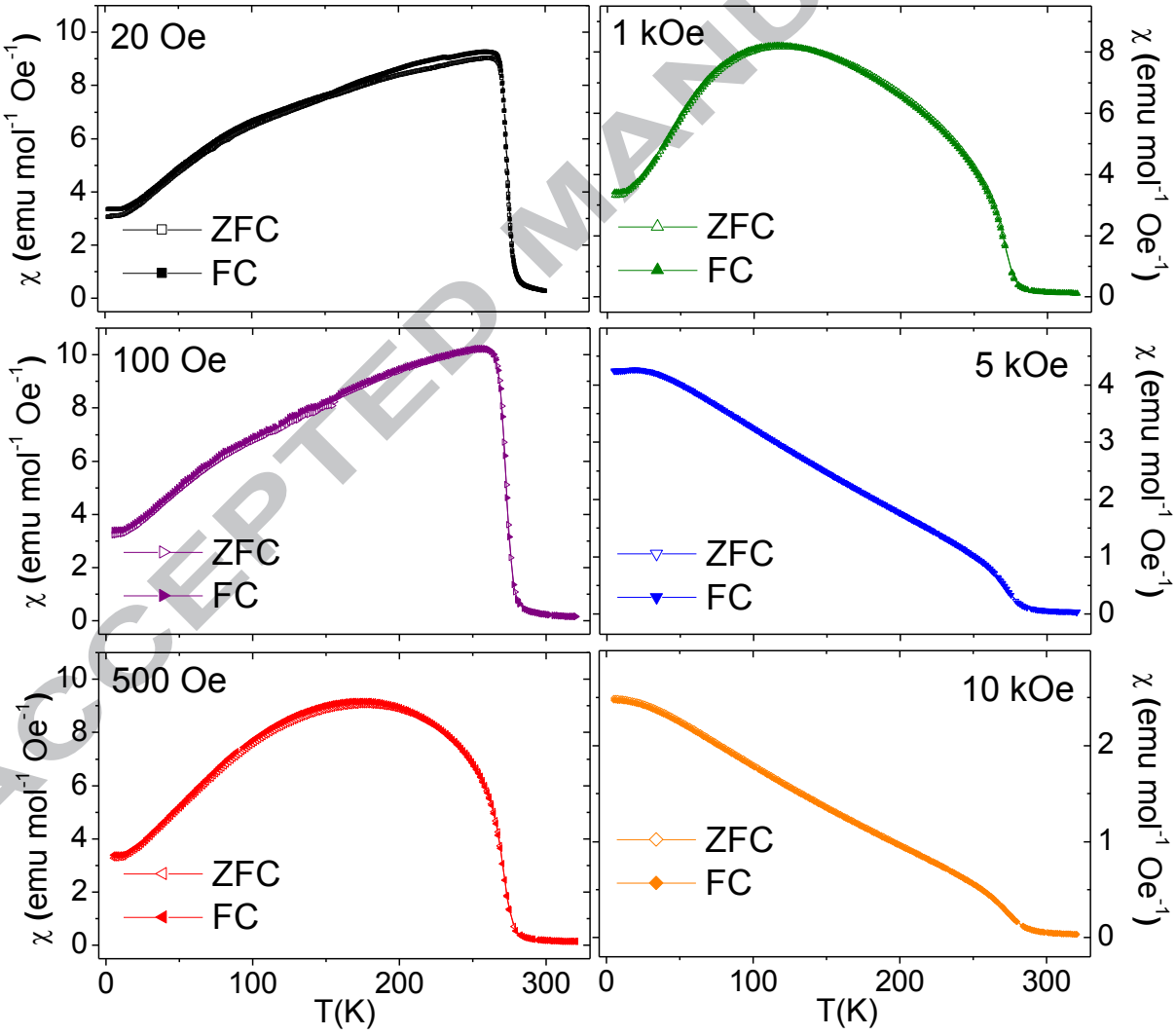

Figure 3 Magnetic susceptibility χ (emu mol^{-1} Oe^{-1}) vs T (K) curves for different applied H (Oe), measured under ZFC and FC conditions as indicated. ZFC and FC curves are approximately identical.

In this context it should be noted that an abrupt spin-reorientation at 50 K had been claimed previously in ilmenite Mn_2FeSbO_6 [22], whereas the data shown here suggest a scenario of more gradual and continuous variations that depend on H and T. It should be further noted that variations in the χ vs T curves in different ilmenite Mn_2FeSbO_6 samples have been previously associated with the crystal quality and phase purity [28], whereas these variations are suggested here to be intrinsic and the competition between different magnetic exchange interactions may play the determining role. In previous research a deviation of ZFC and FC curves had been observed at low H = 20 Oe [28, 32], which cannot be confirmed here.

The magnetization data are summarized in Figure 4 in terms of M (μ_B) vs T (K). The figure inset shows differentiated curves of dM/dT (μ_B/K), where the peak associated with the ferrimagnetic transition is visible consistently at $T_N \approx 270$ K and no clear changes with H are obvious. The mean peak temperature is 272 K, which can be associated with the precise H-independent T_N value. The zero crossings of the differentiated curves in the Figure 4 inset correspond to the maxima in M vs T and χ vs T curves.

The highest overall value in the of M (μ_B) vs T curve in the main Figure 4 at 10 kOe is $\approx$ 4.5 μ_B, which is still below the theoretical maximum of 5 μ_B. Despite the saturation effect demonstrated at higher H, the magnetization may still not be completely saturated even at 10 kOe.

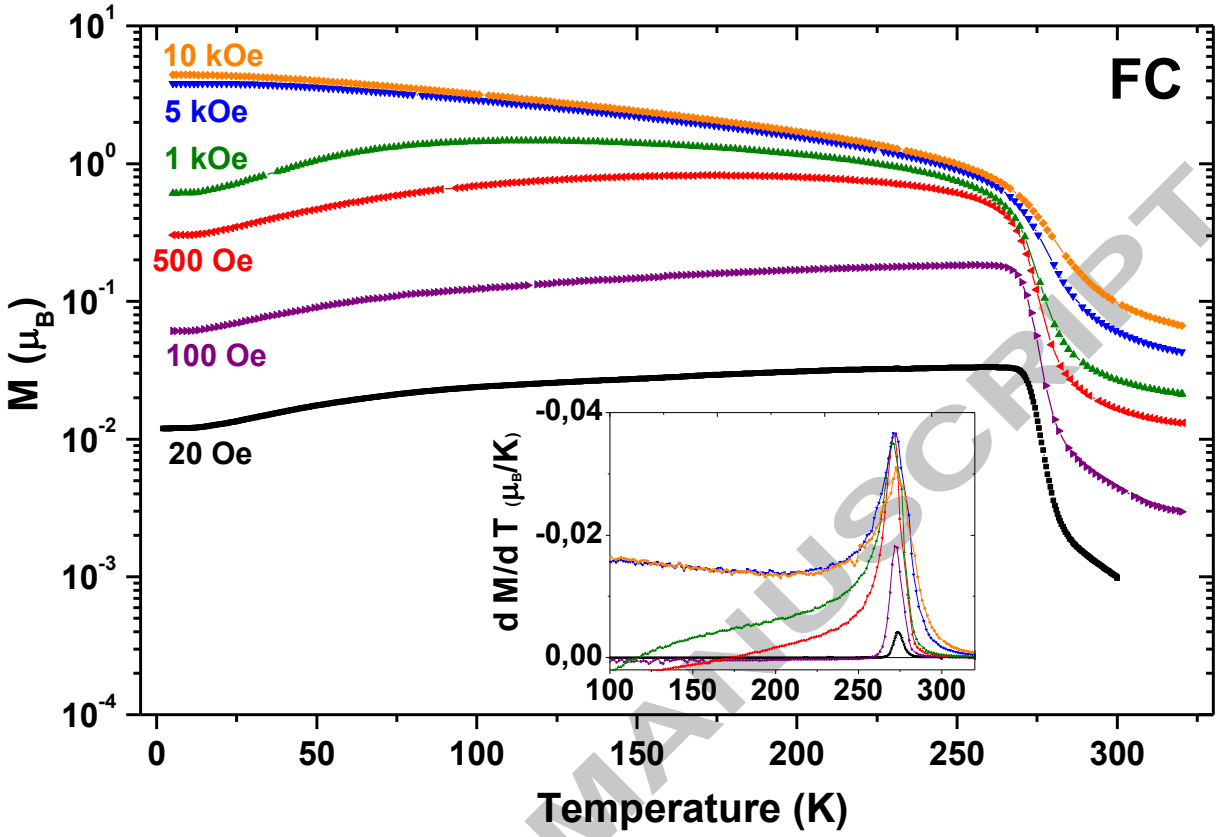

Figure 4 Magnetization M (μ_B) vs T (K) for all applied H (Oe), measured under FC conditions. The inset shows differentiated M vs T curves, i.e. dM/dT (μ_B /K) vs T (K).

Figure 5 shows plots of magnetization M (μ_B) vs applied magnetic field H (Oe) at several selected T, where M never shows full saturation. This is quite clear at T = 200 K and above, but also at the lowest T = 5 K, M still slightly increases up to the highest H = 50 kOe and never reaches the maximum possible moment of 5 μ_B per f.u. This trend was confirmed on M vs H measurements at 50 K, 100 K and 250 K up to H = ±120 kOe (data not shown). These data show exactly the same qualitative features with the same trends but extended to higher H, and the magnetic moments still do not reach the full saturation of 5 μ_B per f.u.

It can be concluded that the saturation of the magnetic moments quite strongly increases with decreasing *T*, but only slightly increases with *H*. However, full saturation cannot be achieved even at *H* = 120 kOe and *T* = 5 K.

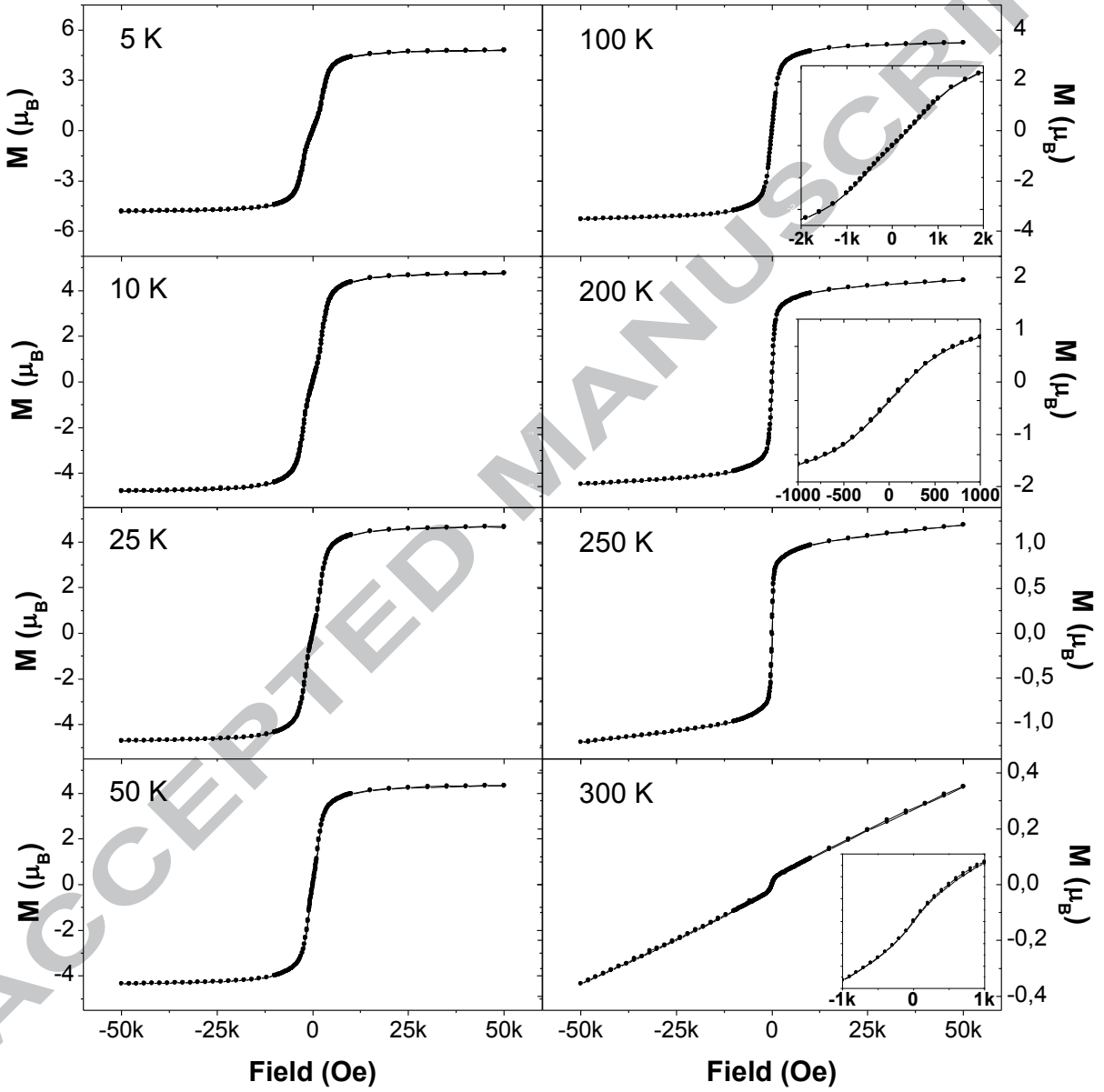

Figure 5 Magnetization *M* (μ_B) vs applied *H* (Oe) curves at different *T* (K) as indicated. *M* was measured by cycling *H* from +50 kOe to -50 kOe and back to + 50 kOe. A near-zero coercive field H_C is indicated.

Figure 5 also demonstrates that the coercive field H_C appears to be always approximately zero or near-zero within the resolution limits of the measurements of ≈ 20 Oe and the magnetization curves measured upon increasing and decreasing H are approximately identical.

The low or zero H_C indicates a very soft ferrimagnetic moment, but the experimental resolution however may not be sufficient to safely confirm the occurrence of superparamagnetism where the coercive fields would be expected to be zero or near-zero. Still, superparamagnetism may be likely to occur, since it has been observed previously in nano-sized α-Fe_2O_3 [48] and it is in fact exclusively reported in ferrites [49] and related binary ferrite compounds [50, 51]. In α-Fe_2O_3 ferrite the Fe^{3+} cations are situated at equivalent B-lattice sites as is the case in Mn_2FeSbO_6, whereas the A-sites in Mn_2FeSbO_6 are occupied by Mn^{2+} and in corundum α-Fe_2O_3 by isoelectronic Fe^{3+} cations. Thus, the two cases may be somewhat comparable. However, there is the clear difference of the B-site Fe^{3+} magnetism in Mn_2FeSbO_6 being diluted by Sb, which should be taken into account, and indeed the magnetic ordering temperature in Mn_2FeSbO_6 (T_N ≈ 270 K) is considerably lower as compared to bulk α-Fe_2O_3 (T_N ≈ 955 K).

The alternative explanation of a very soft magnetic component without the occurrence of superparamagnetism may be less likely, because very soft magnetism is usually observed in ferromagnetic perovskite manganites, but not in ferrimagnetic ilmenites. Therefore, further investigations may be useful to confirm the indications for superparamagnetism encountered here. It should also be noted the possibility that the ferrimagnetic transition at T_N ≈ 270 K and the strong ME coupling effect at ≈ 260 K [22] in ilmenite Mn_2FeSbO_6

could be related with the spin-reorientation at the Morin temperature T_M = 260 K in α-Fe_2O_3 [40, 41, 48].

Figure 5 further indicates a small magnetic anomaly near zero field at 5 K, 10 K, 25 K, 50 K and 100 K, which suggests the presence of an additional magnetic component. This may be associated with a magnetic impurity like MnO, which had been detected previously from neutron diffraction data below 120 K [22]. The Figure 5 insets for 100 K and 200 K indicate that the anomaly is visible at 100 K but not at 200K, and it may therefore be compatible with a MnO impurity. Furthermore, the paramagnetic M vs H curve above T_N at 300 K (Figure 5) shows indications for another magnetic anomaly near zero field, which could be associated with additional magnetic impurities like the potential secondary phase of spinel $MnFe_2O_4$ with $T_N \approx 570$ K, depending on particl e size [52-54]. However, the magnetic signals of this phase were reported to be absent in neutron diffraction data [22], and an alternative explanation may be a residual magnetic moment. This residual magnetic moment would also show near-zero coercive field H_C (see Figure 5 inset of the 300 K curve) and disappears near the satellite peak of the ferroelectric transition in ε' vs T at $T \approx$ 500 K [22]. On a rather speculative note this residual moment could be associated with local B-site Fe^{3+} - Fe^{3+} interactions, considering the following arguments: (i) Fe^{3+} and Sb^{5+} cations are randomly distributed on the ilmenite B-sites and thus, (ii) local Fe^{3+} clusters may form. (iii) Fe^{3+} - Fe^{3+} interactions on the B-sites may persist at higher T at least on a local level as is the case in α-Fe_2O_3 ($T_N \approx 955$ K).

5. Conclusions

The synthetic melanostibite Mn_2FeSbO_6 with ilmenite structure displays a very soft magnetic component below the ferrimagnetic transition at $T_N \approx 270$ K, possibly related with superparamagnetism. The curves of magnetic susceptibility χ vs T display clear signs of weakly H- and strongly T-dependent spin reorientations, which occur gradually and continuously over wide H- and T-ranges. No signs were detected of an abrupt spin reorientation at 50 K as reported previously [22]. The determination of the exact MEC mechanism in ilmenite Mn_2FeSbO_6 may require further investigation, but the fact that a low magnetic field H is sufficient to trigger the MEC [22] may well be related with the near-zero coercive field H_C detected here.

Acknowledgments

This work was supported by the Spanish MINECO under Grant MAT2014-52405-C2-2-R. The author wishes to thank Mar García Hernandez, Federico Mompean and Jesús Prado-Gonjal for allowing use and help with the magnetization measurement equipment.

Declaration of interest statement.

The author declares no conflict of interests.

References

[1] M. Fiebig, Revival of the magnetoelectric effect, Journal of Physics D: Applied Physics, 38 (2005) R123.
[2] R. Ramesh, Emerging routes to multiferroics, Nature, 461 (2009) 1218.
[3] N.A. Hill, Why Are There so Few Magnetic Ferroelectrics?, J. Phys. Chem. B, 104 (2000) 6694.
[4] D.I. Khomskii, Magnetism and ferroelectricity: why do they so seldom coexist?, Bull. Am. Phys. Soc. C (2001) 21.002.
[5] D.I. Khomskii, Classifying multiferroics: Mechanisms and effects, Physics, 2 (2009) 20.
[6] J. Wang, J. Neaton, H. Zheng, V. Nagarajan, S.B. Ogale, B. Liu, D. Viehland, V. Vaithyanathan, D.G. Schlom, U. Waghmare, N.A. Spaldin, K.M. Rabe, M. Wuttig, R. Ramesh, Epitaxial $BiFeO_3$ Multiferroic Thin Film Heterostructures, Science, 299 (2003) 1719.
[7] G. Catalan, J.F. Scott, Physics and Applications of Bismuth Ferrite, Advanced Materials, 21 (2009) 2463-2485.

[8] R. Schmidt, J. Ventura, E. Langenberg, N.M. Nemes, C. Munuera, M. Varela, M. Garcia-Hernandez, C. Leon, J. Santamaria, Magnetoimpedance spectroscopy of epitaxial multiferroic thin films, Physical Review B, 86 (2012) 035113.
[9] Z.V. Gareeva, K.A. Zvezdin, A.P. Pyatakov, A.K. Zvezdin, Novel type of spin cycloid in epitaxial bismuth ferrite films, Journal of Magnetism and Magnetic Materials, 469 (2019) 593-597.
[10] B. Yotburut, P. Thongbai, T. Yamwong, S. Maensiri, Synthesis and characterization of multiferroic Sm-doped $BiFeO_3$ nanopowders and their bulk dielectric properties, Journal of Magnetism and Magnetic Materials, 437 (2017) 51-61.
[11] T. Kimura, S. Kawamoto, I. Yamada, M. Azuma, M. Takano, Y. Tokura, Magnetocapacitance effect in multiferroic $BiMnO_3$, Physical Review B, 67 (2003) 180401(R).
[12] R. Schmidt, W. Eerenstein, T. Winiecki, F.D. Morrison, P.A. Midgley, Impedance spectroscopy of epitaxial multiferroic thin films, Phys. Rev. B, 75 (2007) 245111.
[13] R. Schmidt, W. Eerenstein, P.A. Midgley, Large dielectric response to the paramagnetic-ferromagnetic transition (T_C ~ 100 K) in multiferroic $BiMnO_3$ epitaxial thin films, Phys. Rev. B, 79 (2009) 214107.
[14] L.-J. Zhai, H.-Y. Wang, The magnetic and multiferroic properties in $BiMnO_3$, Journal of Magnetism and Magnetic Materials, 426 (2017) 188-194.
[15] E. Langenberg, I. Fina, J. Ventura, B. Noheda, M. Varela, J. Fontcuberta, Dielectric properties of $(Bi_{0.9}La_{0.1})_2NiMnO_6$ thin films: Determining the intrinsic electric and magnetoelectric response, Physical Review B, 86 (2012) 085108.
[16] E. Langenberg, L. Maurel, N. Marcano, R. Guzmán, P. Štrichovanec, T. Prokscha, C. Magén, P.A. Algarabel, J.A. Pardo, Controlling the Electrical and Magnetoelectric Properties of Epitaxially Strained $Sr_{1-x}Ba_xMnO_3$ Thin Films, Advanced Materials Interfaces, 4 (2017) n/a-n/a.
[17] P. Chen, B.-G. Liu, Giant ferroelectric polarization and electric reversal of strong spontaneous magnetization in multiferroic Bi_2FeMoO_6, Journal of Magnetism and Magnetic Materials, 441 (2017) 497-502.
[18] E. Langenberg, M. Varela, M.V. García-Cuenca, C. Ferrater, M.C. Polo, I. Fina, L. Fàbrega, F. Sánchez, J. Fontcuberta, Epitaxial thin films of $(Bi_{0.9}La_{0.1})_2NiMnO_6$ obtained by pulsed laser deposition, Journal of Magnetism and Magnetic Materials, 321 (2009) 1748-1753.
[19] T. Kimura, T. Goto, H. Shintani, K. Ishizaka, T. Arima, Y. Tokura, Magnetic control of ferroelectric polarization, Nature, 426 (2003) 55-58.
[20] N. Hur, S. Park, P.A. Sharma, J.S. Ahn, S. Guha, S.W. Cheong, Electric polarization reversal and memory in a multiferroic material induced by magnetic fields, Nature, 429 (2004) 392.
[21] R. Vilarinho, E. Queirós, D.J. Passos, D.A. Mota, P.B. Tavares, M. Mihalik Jr, M. Zentkova, M. Mihalik, A. Almeida, J.A. Moreira, On the ferroelectric and magnetoelectric mechanisms in low Fe^{3+} doped $TbMnO_3$, Journal of Magnetism and Magnetic Materials, 439 (2017) 167-172.
[22] A.J. Dos santos-García, E. Solana-Madruga, C. Ritter, A. Andrada-Chacón, J. Sánchez-Benítez, F.J. Mompean, M. Garcia-Hernandez, R. Sáez-Puche, R. Schmidt, Large Magnetoelectric Coupling Near Room Temperature in Synthetic Melanostibite Mn_2FeSbO_6, Angewandte Chemie International Edition, 56 (2017) 4438-4442.
[23] L.J. Igelström, Melanostibian, ein neues Mineral von der Mangangrube Sjögrufvan, Kirchspiel Grythyttan, Gouvernement Örebro, Schweden, Z. Kristallogr., 21 (1893) 246.
[24] L.J. Igelström, Mineralogiska meddelanden - 18. Melanostibian, ett nytt antimonmineral fr°an Sjögrufvan, GFF, 14 (1892) 583.
[25] P.B. Moore, Substitutions of the type $(Sb_{0.5}^{5+}Fe_{0.5}^{3+})$<->$(Ti^{4+})$: The crystal structure of melanostibite, Am. Mineral., 53 (1968) 1104.
[26] P.B. Moore, Contributions to Swedish Mineralogy. II. Melanostibite and manganostibite, two unusual antimony minerals, Ark. Mineral. Geol., 4 (1968) 449.
[27] G.V. Bazuev, B.G. Golovkin, N.V. Lukin, N.I. Kadyrova, Y.G. Zainulin, High Pressure Synthesis and Polymorphism of Complex Oxides Mn_2BSbO_6(B= Fe, V, Cr, Ga, Al), Journal of Solid State Chemistry, 124 (1996) 333-337.
[28] R. Mathieu, S.A. Ivanov, G.V. Bazuev, M. Hudl, P. Lazor, I.V. Solovyev, P. Nordblad, Magnetic order near 270 K in mineral and synthetic Mn_2FeSbO_6 ilmenite, Applied Physics Letters, 98 (2011) 202505.
[29] M. Hudl, R. Mathieu, P. Nordblad, S.A. Ivanov, G.V. Bazuev, P. Lazor, Investigation of the magnetic phase transition and magnetocaloric properties of the Mn_2FeSbO_6 ilmenite, Journal of Magnetism and Magnetic Materials, 331 (2013) 193-197.

[30] G.V. Bazuev, A.V. Korolev, I.V. Nikolaenko, B.G. Golovkin, Synthesis and Magnetic Properties of a New Complex Oxide $Mn_3FeTiSbO_9$ with an Ilmenite Structure, Doklady Chemistry, 462 (2015) 141.
[31] G.V. Bazuev, A.V. Korolev, B.G. Golovkin, Dilute ferrimagnetism of ilmenites $Mn_3FeTiSbO_9$ and $Mn_4FeTi_2SbO_{12}$, Physics of the Solid State, 58 (2016) 1332-1338.
[32] R. Mathieu, S.A. Ivanov, I.V. Solovyev, G.V. Bazuev, P. Anil Kumar, P. Lazor, P. Nordblad, Mn_2FeSbO_6: A ferrimagnetic ilmenite and an antiferromagnetic perovskite, Physical Review B, 87 (2013) 014408.
[33] G. Shirane, S. J. Pickart, Y. Ishikawa, Neutron Diffraction Study of Antiferromagnetic $MnTiO_3$ and $NiTiO_3$, Journal of the Physical Society of Japan, 14 (1959) 1352-1360.
[34] J. Akimitsu, Y. Ishikawa, Y. Endoh, On the two-dimensional antiferromagnetic character of $MnTiO_3$, Solid State Communications, 8 (1970) 87-90.
[35] Y. Todate, Y. Ishikawa, K. Tajima, S. Tomiyoshi, H. Takei, Spin Dynamics in a Quasi-Two Dimensional Antiferromagnet $MnTiO_3$, Journal of the Physical Society of Japan, 55 (1986) 4464-4476.
[36] M. Ye, D. Vanderbilt, Domain walls and ferroelectric reversal in corundum derivatives, Physical Review B, 95 (2017) 014105.
[37] M. Modak, N. Pal, S. Mondal, M. Sardar, S. Banerjee, Magnetic behavior of nanostructured $NiTiO_3$ and NiO material: Anomalous increase in coercivity, Journal of Magnetism and Magnetic Materials, 448 (2018) 221-227.
[38] A.H. Hill, F. Jiao, P.G. Bruce, A. Harrison, W. Kockelmann, C. Ritter, Neutron Diffraction Study of Mesoporous and Bulk Hematite, α-Fe_2O_3, Chemistry of Materials, 20 (2008) 4891-4899.
[39] S. Giri, S. Samanta, S. Maji, S. Ganguli, A. Bhaumik, Magnetic properties of α-Fe_2O_3 nanoparticle synthesized by a new hydrothermal method, Journal of Magnetism and Magnetic Materials, 285 (2005) 296-302.
[40] R.N. Bhowmik, A. Saravanan, Surface magnetism, Morin transition, and magnetic dynamics in antiferromagnetic α-Fe_2O_3 (hematite) nanograins, Journal of Applied Physics, 107 (2010) 053916.
[41] N. Yamamoto, The Shift of the Spin Flip Temperature of α-Fe_2O_3 Fine Particles, Journal of the Physical Society of Japan, 24 (1968) 23-28.
[42] F. Bødker, M.F. Hansen, C.B. Koch, K. Lefmann, S. Mørup, Magnetic properties of hematite nanoparticles, Physical Review B, 61 (2000) 6826-6838.
[43] J. Prado-Gonjal, R. Schmidt, J.-J. Romero, D. Avila, U. Amador, E. Moran, Microwave-Assisted Synthesis, Microstructure, and Physical Properties of Rare-Earth Chromites, Inorganic Chemistry, 52 (2013) 313-320.
[44] Y.L. Su, J.C. Zhang, L. Li, Z.J. Feng, B.Z. Li, Y. Zhou, S.X. Cao, Novel Magnetization Induced by Phase Coexistence in Multiferroic $HoCrO_3$ Chromites, Ferroelectrics, 410 (2010) 102-108.
[45] Y.L. Su, J.C. Zhang, Z.J. Feng, L. Li, B.Z. Li, Y. Zhou, Z. Chen, S.X. Cao, Magnetization reversal and Yb^{3+}/Cr^{3+} spin ordering at low temperature for perovskite $YbCrO_3$ chromites, Journal of Applied Physics, 108 (2010) 013905.
[46] C. Moure, O. Peña, Magnetic features in $REMeO_3$ perovskites and their solid solutions (RE=rare-earth, Me=Mn, Cr), Journal of Magnetism and Magnetic Materials, 337-338 (2013) 1-22.
[47] B.B. Dash, S. Ravi, Sign reversal of magnetization in Mn substituted $SmCrO_3$, Journal of Magnetism and Magnetic Materials, 405 (2016) 209-213.
[48] R. Zboril, M. Mashlan, D. Petridis, Iron(III) Oxides from Thermal Processes: Synthesis, Structural and Magnetic Properties, Mössbauer Spectroscopy Characterization, and Applications, Chemistry of Materials, 14 (2002) 969-982.
[49] D.K. Kim, Y. Zhang, W. Voit, K.V. Rao, M. Muhammed, Synthesis and characterization of surfactant-coated superparamagnetic monodispersed iron oxide nanoparticles, Journal of Magnetism and Magnetic Materials, 225 (2001) 30-36.
[50] M. Virumbrales, V. Blanco-Gutiérrez, A. Delgado-Cabello, R. Sáez-Puche, M.J. Torralvo, Superparamagnetism in $CoFe_2O_4$ nanoparticles: An example of a collective magnetic behavior dependent on the medium, Journal of Alloys and Compounds, 767 (2018) 559-566.
[51] O. Karaagac, B.B. Yildiz, H. Köçkar, The influence of synthesis parameters on one-step synthesized superparamagnetic cobalt ferrite nanoparticles with high saturation magnetization, Journal of Magnetism and Magnetic Materials, 473 (2019) 262-267.
[52] K. Naito, H. Inaba, H. Yagi, Heat capacity measurements of $Mn_xFe_{3-x}O_4$, Journal of Solid State Chemistry, 36 (1981) 28-35.

[53] J.M. Hastings, L.M. Corliss, Neutron Diffraction Study of Manganese Ferrite, Physical Review, 104 (1956) 328-331.
[54] J.P. Chen, C.M. Sorensen, K.J. Klabunde, G.C. Hadjipanayis, E. Devlin, A. Kostikas, Size-dependent magnetic properties of $MnFe_2O_4$ fine particles synthesized by coprecipitation, Physical Review B, 54 (1996) 9288-9296.

Figure captions

Figure 1 Crystal structure of ilmenite Mn_2FeSbO_6 according to [25]: **(a)** Structural [110] projection. The stacking of Mn-Sb/Fe cation layers along the [001] ***c***-direction is indicated. **(b)** Cations are slightly shifted from the octahedral centers as indicated by slightly different Mn-O and Fe/Sb – O bonding distances due to Coulomb repulsions between Mn^{2+} and Fe^{3+}/Sb^{5+} cation pairs, indicated by blue dashed lines. **(c)** Hexagonal arrangement of the octahedra within the (001) ***c***-planes demonstrating the vacant sites □.

Figure 2 Hexagonal sub-cells of Mn_2FeSbO_6 ilmenite. The magnetic spin exchange interactions between isoelectronic Mn^{2+} cations (orange spheres) and Fe^{3+} (green) are depicted. Non-magnetic Sb^{5+} cations are shown in black, □ are vacant sites. Red arrows indicate possible spin orientations and black arrows show the cationic displacements due to Coulomb repulsions (blue dashed lines).

Figure 3 Magnetic susceptibility χ (emu mol^{-1} Oe^{-1}) vs T (K) curves for different applied H (Oe), measured under ZFC and FC conditions as indicated. ZFC and FC curves are approximately identical.

Figure 4 Magnetization M (μ_B) vs T (K) for all applied H (Oe), measured under FC conditions. The inset shows differentiated M vs T curves, i.e. dM/dT (μ_B /K) vs T (K).

Figure 5 Magnetization M (μ_B) vs applied H (Oe) curves at different T (K) as indicated. M was measured by cycling H from +50 kOe to -50 kOe and back to + 50 kOe. A near-zero coercive field H_C is indicated.